Electronic Supplementary Information

Self-assembled rhomboidal ammonia monolayer confined in two vertically stacked graphene oxide/graphene nanosheets

Zhi-Bin Jian,[a] Jie Bie[ab] and Shuang Chen[a]*

[a]Kuang Yaming Honors School and Institute for Brain Sciences, Nanjing University, Nanjing, Jiangsu 210023, China

[b]National Laboratory of Solid State Microstructures and Department of Physics, Nanjing University, Nanjing, Jiangsu 210093, China

E-mail: chenshuang@nju.edu.cn

S1. Building of computational slab models

In order to locate possible NH_3 phases confined in two packed graphene oxide (GO)/graphene (G) nanosheets, three NH_3s@GO model systems are constructed in consideration of various oxygen-containing groups in two-dimensional (2D) GO nanosheets, and one NH_3s@G model system is also built for comparison. In these model systems, only NH_3 monolayers are deposited into two confining planes. The oxygen-containing functional groups in GO sheets are diverse, and their components and contents which significantly depend on the synthetic methods are difficult to be determined.[S1] The previous experimental observation has predicted that the main oxygen-containing functional groups of GO are hydroxyl, epoxy, ether, and carbonyl in the basal plane and hydroxyl and carboxyl at the edge.[S1, S2] Herein, we refer to the experimental observation and then build three GO monolayers including the hydroxyl/carbonyl-, epoxy-, and ether-functionalized ones in **Fig. S1a-c** respectively. And we also take the pure graphene layer without oxygen-containing groups as a model system in **Fig. S1d**. Among these GO monolayers, the sp^2-carbon skeleton of hydroxyl/carbonyl-functionalized GO is seriously destroyed due to introduction of hydroxyl and carbonyl groups, but this monolayer may greatly approach to the real one. These hydrophilic and hydrophobic GO/G monolayers are vertically stacked to confine NH_3 monolayers to generate our studied slab models of NH_3s@GO/G with a *c*-axis length of 60 Å to ensure the thick-enough vacuum layer of about 50 Å, also in sufficient consideration of size match between 2D confining planes and NH_3 monolayer. The corresponding lattice parameters are summarized in **Table S1**. For four kinds of slab models, their *a*-axis lengths range from 7.13 Å to 9.92 Å and their b-axis lengths changes from 8.52 Å to 10.8 Å. Although theses lattice lengths in 2D planes change a lot because of introducing various O-bearing functional groups or not, the NH_3 molecules are deposited into these side-different four GO/G bilayers to form a monolayer with molecular number fixed referring to the density of solid NH_3[S3] so that the surface densities of NH_3 monolayers in different models vary from 0.075 to 0.13 $Å^{-2}$. Noticeably, their

oxygen-containing groups of GO bilayers are set to point to the filled NH_3 molecules. For the confined NH_3 molecules, two cases, ordered and amorphous NH_3 monolayers, are considered for their initial configurations. The ordered NH_3 monolayer as mentioned above refers to the crystal structure of solid NH_3,[S3] since the crystal structure of liquid NH_3 is quite close to that of solid NH_3, only with a little longer lattice constants.[S4] The interlayer space of each NH_3s@GO/G is set to be large enough to let each NH_3 monolayer relax into its possible solid or liquid phases in our first-principles geometry optimization. For comparison, the amorphous NH_3 monolayer is also built just referring to the same surface density. In our first-principles calculations, we only take the amorphous NH_3 monolayer in ether-functionalized GO bilayer (**Fig. S2**) as an example to text the influence of initial configurations of NH_3 monolayers on formation of possible final configurations. Finally, the strain effect on the phase transition of NH_3 monolayer confined in vertically stacked ether-functionalized GO bilayer is investigated by only changing the interlayer spacing of two GO sheets.

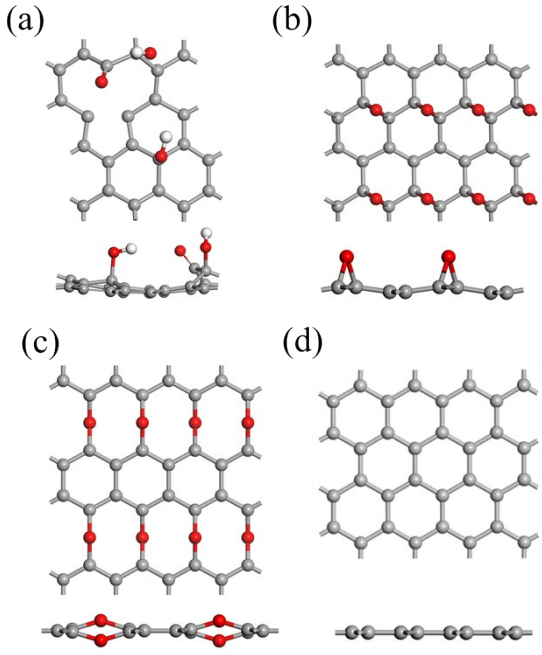

Figure S1. Optimized structures (both top and side views) of 2D (a-c) graphene oxide and (d) graphene monolayers based on the first-principles calculations. The graphene oxide monolayers include (a) hydroxyl/carbonyl-, (b) epoxy-, and (c) ether-functionalized ones.

Table S1. Computational supercell volumes and surface densities of four NH_3s@GO/G models.

Model	Supercell Volume (Å^3)	Surface Density (Å^{-2})
The First-principles Calculations		
NH_3s@hydroxyl/carbonyl-functionalized GO	7.13×8.61×60	0.13
NH_3s@expoxy-functionalized GO	9.84×8.52×60	0.095
NH_3s@ether-functionalized GO	9.92×10.8×60	0.075
NH_3s@G	9.84×8.52×60	0.095
AIMD Simulation		
NH_3s@ether-functionalized GO	14.82×16.19×60	0.075

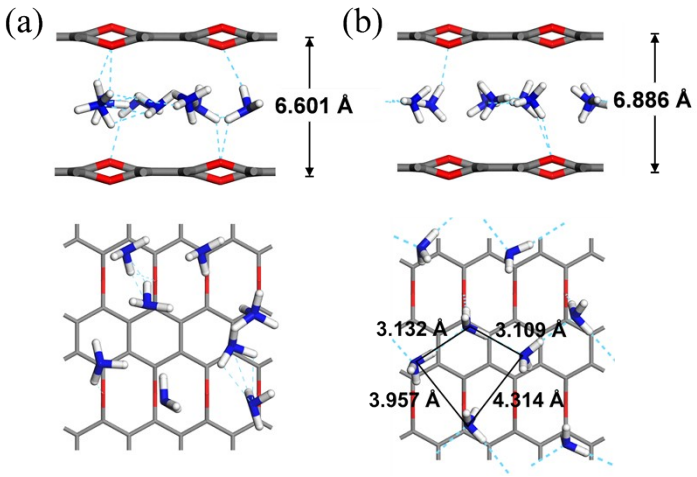

Figure S2. Structures of amorphous NH_3 monolayer confined in two vertically stacked ether-functionalized GO nanosheets for its both side-view and top-view (a) initial structures and (b) optimized structures.

S2. Zigzag hydrogen bonding in NH_3 monolayer highlighted by using Electron Localization Function (ELF) analysis

Taking NH_3s@ether-functionlized GO as a benchmark, the NH_3 monolayer is taken from this benchmark system to estimate its charge density based on the first-principles calculations. Then learning from this charge density results, the ELF analysis[S5] is further performed to highlight hydrogen bonding within this confined NH_3 monolayer (Fig. S3). The possibility of finding a pair of electrons at certain position is colored on a blue-green-red scale according to values ranging from 0 to 1 to reflect the bonding nature of materials, where blue (0) indicates a delocalized electron pair, red (1) indicates a localized electron pair for bonding, and green (0.5) can be viewed as a delocalized one and a localized one for nonbonding. As shown in Fig. S3, the N atom of each NH_3 molecule in this monolayer is located at the center of the green region and also colored in green. Two round red spots with outermost yellow circles indicate two H atoms covalently bonding with N atom. Noticeably, the third bonded H atom is covered by the top H atoms because of Y configuration. The other red spots with yellow outer ring in an irregular shape represents the lone pair electrons of N atom. According to this ELF picture, we can recognize one N-H bond of a NH_3 molecule in this (001) surface faces to the lone pair electrons of N atom of the neighboring NH_3 molecule to form a hydrogen bond. Because of sp^3 hybridization of N atom that determines the spatial distribution of lone pair electrons and bonding electrons of each NH_3 molecule, these neighboring NH_3 molecules form the zigzag hydrogen bonding alignment in the confined NH_3 monolayer finally highlighted by this ELF picture.

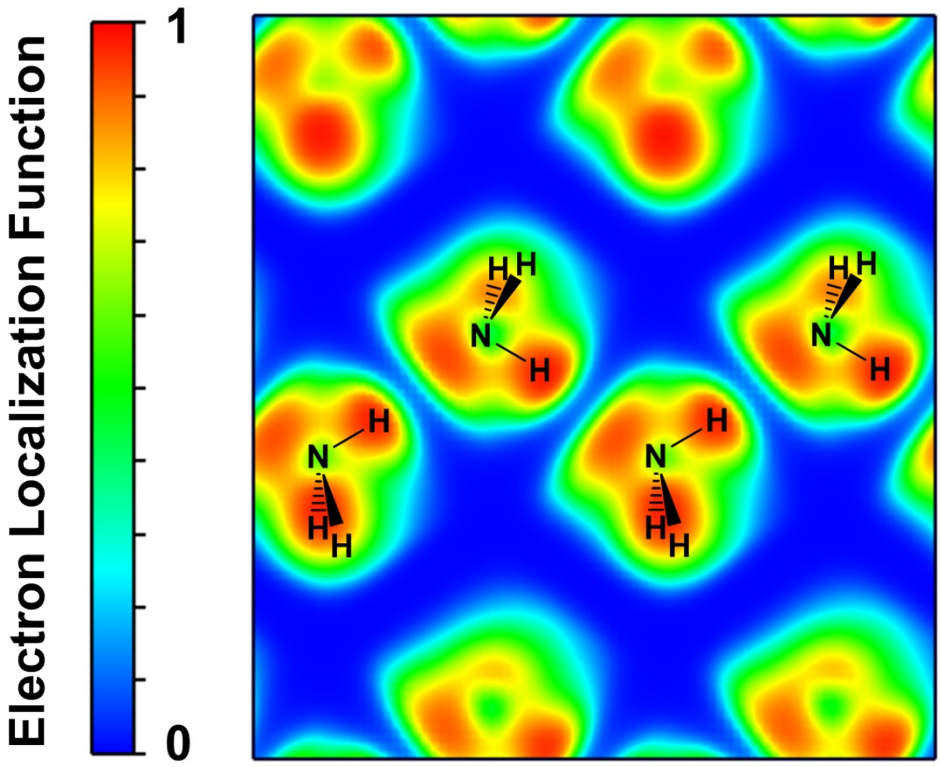

Figure S3. ELF analysis of NH_3 monolayer taken from NH_3s@ether-functionalized GO viewed along (001) surface. NH_3 molecules are highlighted to distinguish the bonding nature. A color-bar is given to present ELF values.

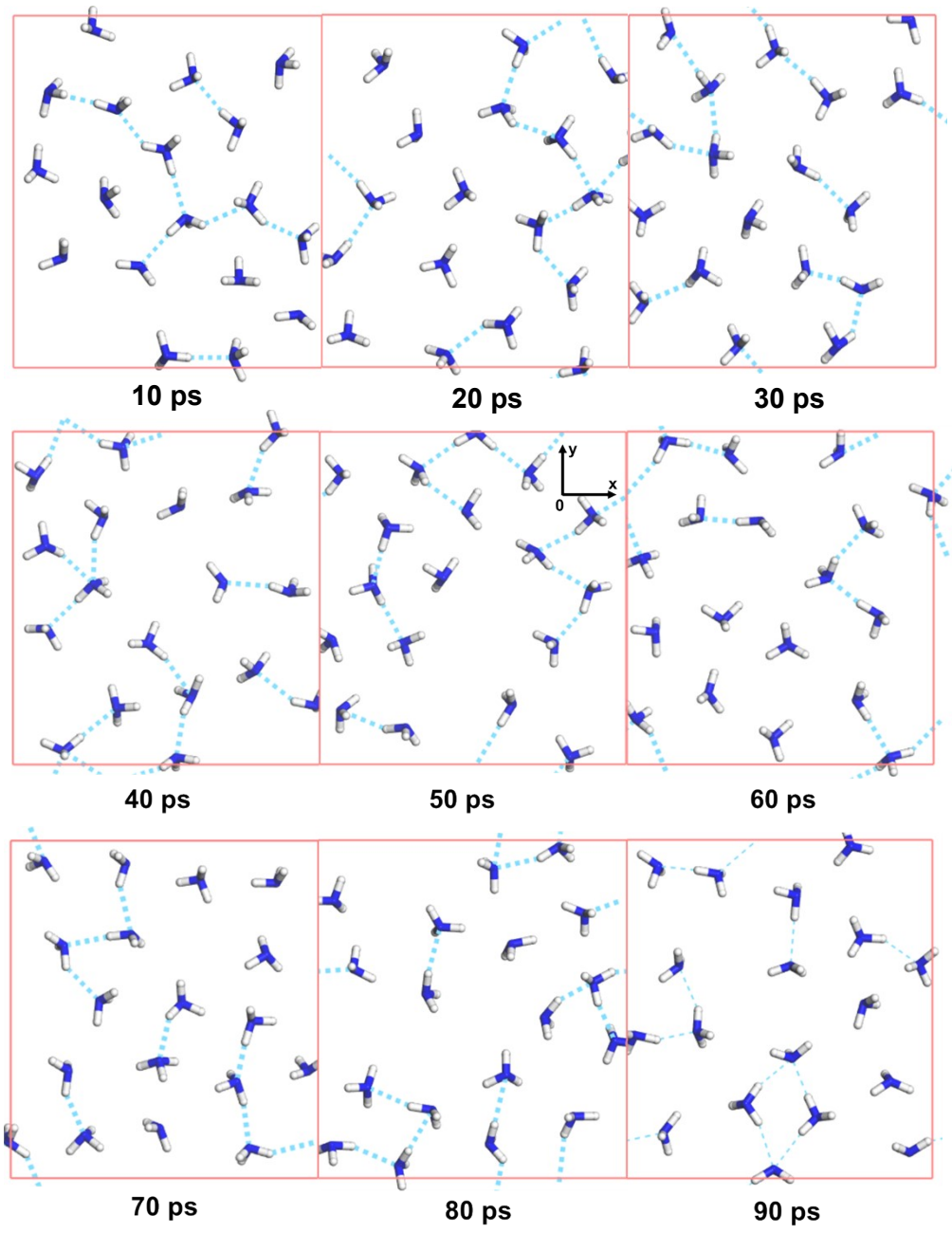

Figure S4. Selected snapshots of NH_3s@ether-functionalized GO learning from the trajectory of its AIMD simulation. The surface axes (*x* and *y*) in 2D plane are also highlighted in insets.

S3. Choice of London dispersion corrections in density function theory (DFT) calculations for our studied systems

We know DFT-D3 is an update of DFT-D2, and it is now the most widely used DFT-D method since it has refined regarding higher accuracy, broader range of applicability, and less empiricism compared to DFT-D2.[S6] In our first-principles calculations and AIMD simulations, the D3 London dispersion corrections combined with the PBE functional is chosen to well consider intermolecular interactions in our studied systems, NH_3 molecules confined in two GO/G nanosheets. Here, we still make a comparison between PBE-D3 and PBE-D2 functionals by taking geometry optimization of NH_3s@ether-functionalized GO as an example. As shown in Table S2, this geometry optimization comparison starts from the same initial structure. After geometry optimization, the structural parameters of the example system calculated based on PBE-D2 are a little different from those calculated based on PBE-D3. Both functionals predict a rhomboidal NH_3 monolayer with Y-shape molecules. The corresponding side lengths of 2D lattices calculated by using PBD-D3 and PBE-D2 are nearly the same with a little difference not larger than 0.068 Å. But the interlayer spaces are quite different. The one predicted by PBE-D2 is 1.23 Å smaller than that predicted by PBE-D3.

Table S2. Optimized structures of NH_3s@ether-functionalized GO with structural parameters calculated based on (a) PBE-D3 or (b) PBE-D2 functionals in the first-principles calculations for comparison.

DFT Functional	Initial	Optimized	
		Side View	Top View
PBE-D3	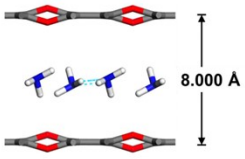	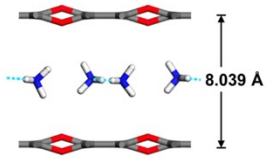	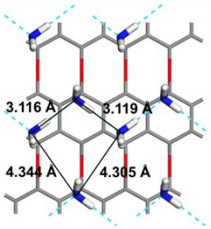
PBE-D2	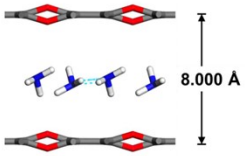	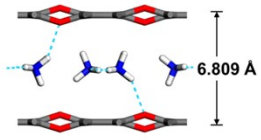	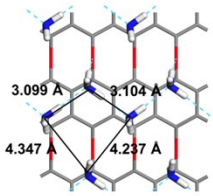

S4. Choice of *k* points

In our first-principles calculations and AIMD simulations, the *Γ* point is used in consideration of computational consuming. We take NH_3s@ether-functionalized GO as an example to test choice of *k* points. As shown in Table S3, this geometry optimization comparison starts from the same initial structure. After geometry optimization, the structural parameters of the example system calculated by using the *k* mesh of 4×4×1 are a little different from those calculated by using the *Γ* point. Both calculations by using different *k* points predict a rhomboidal NH_3 monolayer with Y-shape molecules. The corresponding side lengths of 2D lattices calculated by using *Γ* point and the *k* mesh of 4×4×1 are nearly the same with a little difference not larger than 0.093 Å. But the interlayer spaces are quite different. The one predicted by *Γ* point is 0.98 Å larger than that predicted by the *k* mesh of 4×4×1. We think this choice is economic and accurate.

Table S3. Optimized structures of NH_3s@ether-functionalized GO with structural parameters calculated by Γ point and a *k* mesh of 4×4×1 for comparison.

K Points	Initial	Optimized	
		Side View	Top View
Γ	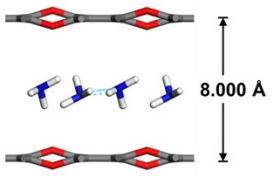	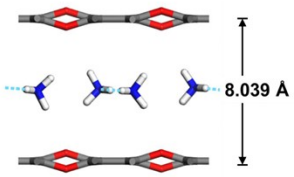	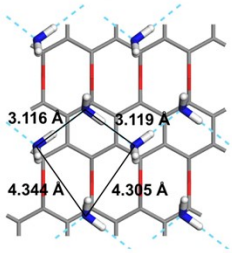
4×4×1	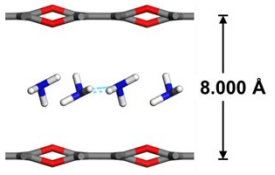	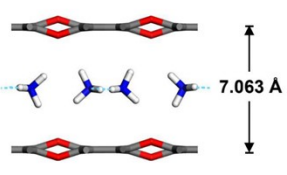	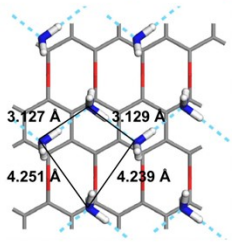

Supplementary references

S1. W. Gao, L. B. Alemany, L. Ci and P. M. Ajayan, *Nat. Chem.*, 2009, **1**, 403-408.

S2. T. Szabó, O. Berkesi, P. Forgó, K. Josepovits and I. Dékány, *Chem. Mater.*, 2006, **18**, 2740-2749.

S3. I. lovsson and D. H. Templeton, *Acta Cryst.*, 1959, **12**, 832–836.

S4. W. L. Jorgensen and M. Ibrahim, *J. Am. Chem. Soc.*, 1980, **102**, 3309-3315.

S5. A. D. Becke and K. E. Edgecombe, *J. Chem. Phys.,*1990, **92,** 5397-5403.

S6. S. Grimme, *WIREs Comput. Mol. Sci.*, 2011, **1**, 211-228.